A FLANN-BASED CONTROLLER FOR MAXIMUM POWER POINT TRACKING IN PV SYSTEMS UNDER RAPIDLY CHANGING CONDITIONS

Lian Lian Jiang[1]*, Douglas L. Maskell*[1]*, and Jagdish C. Patra*[2]

[1]School of Computer Engineering
Nanyang Technological University, Singapore

[2]Faculty of Engineering and Industrial Sciences
Swinburne University of Technology, Australia

ABSTRACT

In order to increase the efficiency of the Photovoltaic (PV) system, the PV system should be operated at the Maximum Power Point (MPP). The MPP Tracking (MPPT) is an essential part in achieving this improvement. Some of the existing techniques such as Perturb-and-Observe (P&O) and Incremental Conductance (INC) are relatively simpler to implement, but under rapidly changing irradiance and temperature conditions, they fail to track the MPP. Although methods such as Multilayer Perceptron (MLP) and Fuzzy Logic (FL) are efficient in tracking the MPP, their implementation increases the system complexity. In this paper, we propose a novel artificial intelligence based controller for MPPT, which can efficiently track the MPP, while keeping the computational complexity within the limits. Our technique uses Functional Link Artificial Neural Network (FLANN) to predict the PV output voltage at the MPP. Since there is no hidden layer, FLANN is computationally inexpensive. Simulation results verify that the proposed FLANN controller is computationally less intensive and exhibits higher efficiency under rapidly changing weather conditions.

Index Terms— MPPT, FLANN, PV system, rapidly changing weather condition, computational complexity

1. INTRODUCTION

Due to constantly growing environmental concerns, non-conventional energy sources are attracting more and more global attention. Solar energy systems are of particular interest due to their lower maintenance, abundance of energy source, and advancements in semiconductor and power electronic devices. Solar energy systems directly convert solar radiation into electricity by photovoltaic effect. Assemblies of solar cells make solar modules, and several modules in series or parallel make photovoltaic (PV) array. Due to the nonlinearity between PV output voltage and current, there is a unique MPP in the power-voltage characteristics under uniform weather conditions. In order to maximize the efficiency of photovoltaic systems, their operating point should be at MPP. Therefore, an MPP tracker needs to be set up between the PV array and the load. Fig. 1 schematically shows a common standalone PV system. The MPPT section includes an MPPT controller, control unit, and a Boost DC-DC converter. The MPPT controller outputs the reference voltage for the PV array using different MPPT algorithms. By tuning the duty cycle of the PWM used by the semiconductor switch (IGBT) in the DC-DC converter, PV terminal voltage is adjusted, so that the PV system works at the MPP.

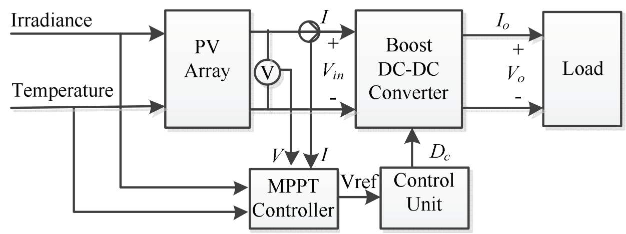

Fig. 1. Schematic diagram of the PV system.

Over the past few years, researchers have proposed several MPPT algorithms, such as Perturb-and-Observe (P&O) [1], Constant Voltage Tracking (CVT) [2], Incremental Conductance (INC) [3], Artificial Neural Network (ANN) [4], Fuzzy Logic (FL) [5], and other modified algorithms based on these methods. Among these, P&O and INC are very popular in commercial electrical products and are efficient under uniform weather conditions, but they fail to follow the MPP under rapidly changing weather conditions. For example, the principle of P&O is to periodically perturb (increase or decrease) PV array terminal voltage and compare instant power $P(k)$ with previous power $P(k\text{-}1)$ to change power output of PV array. When a perturbation gives rise to an increase in the PV array power, the direction of the perturbation is maintained, otherwise it is reversed [6]. In Fig. 2, the PV system starts from point A and the operating point moves from A to C due to the voltage perturbation, δV, under approximately constant atmospheric condition. When the environmental conditions vary rapidly, the power curve changes from P1 to P2. According to the principle of P&O algorithm, if the power increase (δPi) made by the raise of irradiance is larger than the power increase (δPv) made by the voltage perturbation, the next voltage perturbation will continue to increase. However, this direction negates the condition to reach the MPP (point D).

Compared to P&O and INC algorithms, artificial intelligence based methods such as ANN and FL are more efficient and flexible because they can predict the MPP under rapidly changing weather conditions. Whereas, the disadvantages of ANN and FL are that they add complexity to the system implementation and take longer time for network training.

In this paper, we use a novel FLANN-based controller to predict the optimal reference voltage for PV array under rapidly changing environment conditions. FLANN features fast convergence speed, simplicity, and good accuracy [9]. In our previous works, we have successfully used the FLANN in modeling solar cells [7] - [11], and our current work verifies its effectiveness in MPP tracking.

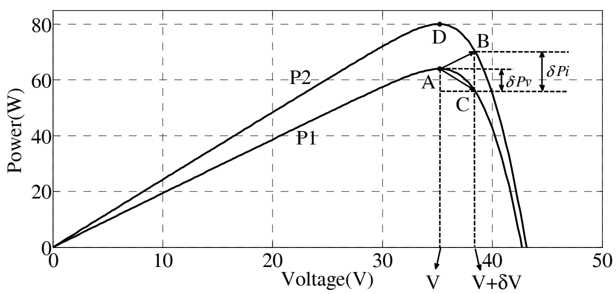

Fig. 2. The P&O fails to determine the right tracking direction to the MPP (adopted from [6]).

2. SYSTEM DESIGN

In this section, we introduce the two-diode PV array model and the fundamental principle of the FLANN.

2.1 Two-diode PV array model

A photovoltaic cell consists of silicon P-N junctions, which convert solar energy directly into electricity by photovoltaic effect. In our work, we use the two-diode model [12] for PV array modeling. It improves accuracy especially under low irradiance and reduces computational time.

We consider that the PV array contains N_{ss} modules in series and N_{pp} modules in parallel. The output current of the PV array is given by the equation [12]

$$\begin{aligned} I = I_{pv}N_{pp} - I_{01}N_{pp}[\exp(\frac{V+\lambda IR_s}{a_1V_tN_{ss}})-1] \\ - I_{02}N_{pp}[\exp(\frac{V+\lambda IR_s}{a_2V_tN_{ss}})-1] - \frac{V+\lambda IR_s}{\lambda R_p} \end{aligned} \tag{1}$$

where I is the photovoltaic output current, V is the photovoltaic output voltage, $\lambda = N_{ss} / N_{pp}$, R_s and R_p are the series and parallel resistances, respectively, V_t is the thermal voltage of the two diodes ($V_t = N_s k\, T / q$), k is the Boltzman constant, q is the electron charge, and a_1, a_2 are the diode ideal constants. The light generated current is given by

$$I_{pv} = (I_{pv\_STC} + K_i(T - T_{STC}))\frac{G}{G_{STC}} \tag{2}$$

where I_{pv_STC} represents the light generated current under standard test conditions (STC) with temperature T_{STC} = 25℃, and irradiance G_{STC} = 1000 (w/m^2), and the constant K_i is the short circuit current coefficient. The reverse saturation current of the diode is given by

$$I_{01} = I_{02} = \frac{I_{sc\_STC} + K_i\Delta T}{\exp((V_{oc\_STC} + K_v\Delta T)/V_t) - 1} \tag{3}$$

where the constant K_v is the open circuit voltage coefficient, I_{sc_STC} is the short circuit current under STC, and V_{oc_STC} is the open circuit voltage under STC. In fact, the equation (1) can be represented as $I = f(I, V)$. Therefore, for a given voltage value, this nonlinear equation is solved using standard Newton-Raphson method. For the converter, by tuning the duty cycle (D_c), the output voltage (V_0) is obtained from its input voltage (V_{in}) by formula $V_0 = V_{in} / (1 - D_c)$.

The PV modules used in this work are SL80CE-36M. They are configured as two PV modules in series with 72 solar cells in series inside each module. The parameters of each module are, maximum power: 80 W, optimum power voltage (V_{mp}): 35.1 V, optimum power current (I_{mp}): 2.28 A, open circuit voltage (V_{oc}): 43.2 V, short circuit current (I_{sc}): 2.44 A, short circuit current coefficient (K_i): 0.976 mA/℃, and open circuit voltage coefficient (K_v): -164.16 mV/℃.

2.2 Principle of the FLANN

The FLANN consists of a functional expansion block (FEB) and a single-layer perceptron network as shown in Fig.3. Irradiance and temperature are the inputs of the PV arrays. The functional expansion block is used to transfer the input variable into a higher dimension space [13]. The expanded inputs are connected to the output layer, which is activated by a hyperbolic tangent transfer function. The purpose of training net is to minimize the cost function to a particular limit by modifying network weights continuously. We used Levenberg - Marquardt (LM) algorithm to train the network.

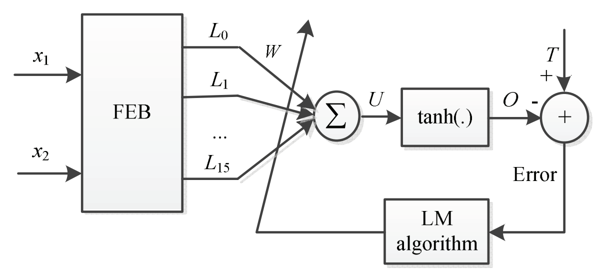

Fig. 3. Schematic diagram of the FLANN.

We denote the inputs (irradiance and temperature) by

$$X = [x_1, x_2]' \tag{4}$$

where X is a input sample with total number of P, and (') denotes transposition. Based on various trials on different functional expansion of trigonometric polynomials, we chose the trigonometric expansions as follows

$$\begin{array}{lll} L_0=1, L_1=x_1x_2 & L_6=x_1\cos(\pi x_1), & L_{11}=x_2\cos(\pi x_2), \\ L_2=x_1, & L_7=x_2, & L_{12}=x_1\cos(\pi x_2), \\ L_3=\sin(\pi x_1), & L_8=\sin(\pi x_2), & L_{13}=x_1\sin(\pi x_2), \\ L_4=\cos(\pi x_1), & L_9=\cos(\pi x_2), & L_{14}=x_2\cos(\pi x_1), \\ L_5=x_1\sin(\pi x_1), & L_{10}=x_2\sin(\pi x_2), & L_{15}=x_2\sin(\pi x_1) \end{array} \tag{5}$$

Thus, the expanded input is $L = [L_0, L_1, L_2, ..., L_{15}]'$. By using LM algorithm, the weights and biases are tuned until the cost function is minimized within a limit. The cost function for the kth sample data is given by

$$E_k = \frac{1}{2}(T_k - O_k)^2 \quad (6)$$

where T_k is the target output and O_k is the network output

$$O_k = f(U_k) = \tanh(U_k) \quad (7)$$

where the input of the hyperbolic tangent transfer function is given by

$$U_k = W_k' L_k \quad (8)$$

where $W_k=[w_{k,0}, w_{k,1}, w_{k,2}, ..., w_{k,15}]'$ is the weight vector for the kth sample.

2.3 Generation of data set for training the network

In our proposed FLANN-based controller, the inputs are irradiance and temperature, and the output is the optimal operating voltage for the PV array. The process of getting optimal operating voltage at different irradiance and temperature conditions are illustrated in Fig. 4. Firstly, the PV array model is built as described in section 2.1. Secondly, the P-V curves for different irradiance and temperature conditions are generated. In the next step, maximum power for each P-V curve is computed and finally, the optimal operating voltages for each P-V curve are obtained.

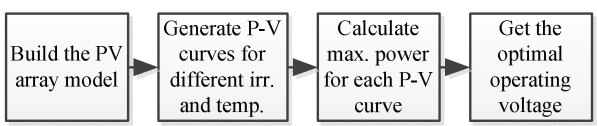

Fig. 4. Process of generating training data sets.

During data generation, temperature is increased by 2℃ per step from 0 to 70℃, and irradiance is added by 50 *w/m*^{2} per step from 0 to 1500 *w/m*^{2}. Thus, 1050 groups of samples are generated. These data are randomly divided into three parts, of which 80% is used for training, 10% for validation, and 10% for testing.

3. EXPERIMENTAL RESULTS

Here, we provide the experimental setup and MPPT performance comparison between FLANN and other algorithms.

3.1 Setup

In order to verify that the FLANN have (i) lower computational complexity than multilayer perceptron (MLP) controller does and (ii) higher efficiency than P&O under rapidly changing irradiance inputs, a PV system was built based on MATLAB and three experiments were conducted as below.

Experiment 1. This experiment compares the computational complexities of FLANN [13] and MLP [4]. The computational complexity is reflected by calculating the average execution time of one iteration during training process. The number of additions, multiplications, tanh(.) and trigonometric expansions can also be evaluated as in [13]. Here, we consider a two-layer MLP with {2 - 8 - 1} and a FLANN with {16 - 1} architecture. Same training parameters are set for both networks. Thirty runs were conducted for each algorithm. Training goal of mean squared error was 0.0005, maximum iterations for training was set to 100, learning rate was 0.2, and other parameters were set with default values.

Experiment 2. This experiment was carried out to compare the efficiency of FLANN, P&O, and MLP under rapidly changing irradiance with a trapezoidal shape. The temperature was set constant at 35℃. The efficiency of the algorithm is calculated as

$$Efficiency = \frac{P_{output}}{P_{ideal}} \times 100\% \quad (9)$$

where P_{ideal} and P_{output} are ideal power output and power output by P&O or by FLANN respectively.

Experiment 3. This experiment was conducted to compare the energy output of FLANN, P&O, and MLP controllers under the real weather conditions. The ideal energy (E_{ideal} (kWh)) and the energy (E_α (kWh)) produced using different algorithms during the time interval, $[t_1, t_2]$, are given by

$$E_{ideal} = \int_{t_1}^{t_2} P_{ideal}dt \ , \ E_\alpha = \int_{t_1}^{t_2} P_\alpha dt \quad (10)$$

The energy loss ($E_{L,\alpha}$) is calculated by

$$E_{L,\alpha} = \frac{E_{ideal} - E_\alpha}{E_{ideal}} \times 100\% \quad (11)$$

3.2 Results

Using the results from Experiment 1, Table 1 shows the comparison of maximum, minimum iterations and average execution time per iteration to train the network. It shows that the training time of FLANN per iteration is about 3.4 times shorter than that by MLP, which means that FLANN gives a faster convergence speed than that by MLP. In addition, the number of average iterations to converge by FLANN is also much less than that by MLP. Due to the absence of hidden layer in FLANN, it is computationally inexpensive. The characteristic of less computational complexity by FLANN than that by MLP can also be found in [13].

Using the results from Experiment 2, Fig. 5 shows that for constant irradiance, such as from 10 sec to 30 sec, all three algorithms exhibit the same performance with efficiency of 94.5%. However, when irradiance changes from 120 *w/m*^{2} to 1000 *w/m*^{2} in 15 seconds from 30 sec to 45 sec, the P&O method fails to follow the transient power and the efficiency falls down from 94.5% to around 55%. Whereas, the FLANN and MLP controllers track this transient process very well with a higher efficiency than stable stage.

Fig. 6 shows the power output under real weather condition obtained from Experiment 3. To highlight the effectiveness of different MPPT controllers under rapid change in irradiance, a magnified portion of Fig. 6 is shown in Fig. 7. We can see that P&O algorithm in green line fails to follow the ideal power line. Whereas, the FLANN and MLP can track the maximum power line very well. Table 2 shows that with an ideal energy output of 0.8867 kWh by the equation (10), the energy loss calculated from (11) reduces by 1.342% and 1.354% using FLANN and MLP respectively. This demonstrates that ANN methods exhibit higher efficiency under rapidly varying weather conditions. The more irradiance transitions, the more effective FLANN based MPPT is. With this improvement, more energy can be saved in a long-term running. For example, for a medium sized PV solar power station with an annual generation of 30 GWh, 402.6 MWh of energy can be saved each year with adoption of FLANN. Therefore, it is favorable to use the FLANN as a MPPT controller in the PV systems if the computational complexity and fast-changing environmental conditions are considered.

Table 1. Comparison of execution characteristics for MLP and FLANN during training process within 30 runs.

ANN type	Network structure	No. of iterations			Avg. execution time / epoch (ms)
		Mean	Max.	Min.	
MLP	2-8-1	13	73	4	219.6
FLANN	16-1	7	12	3	63.8

Table 2. Energy loss of three trackers under real irradiance data.

Algorithm	P&O	MLP	FLANN
Energy (kWh)	0.8481	0.8601	0.8600
Energy Loss (%)	4.3532	2.9999	3.0112

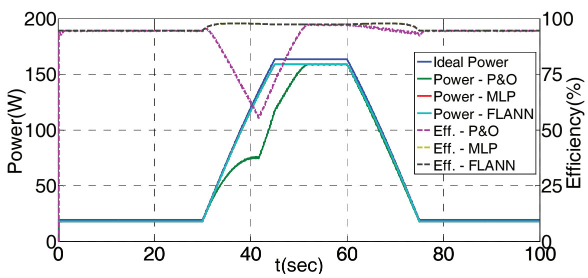

Fig. 5. Power output under irradiance with trapezoidal shape.

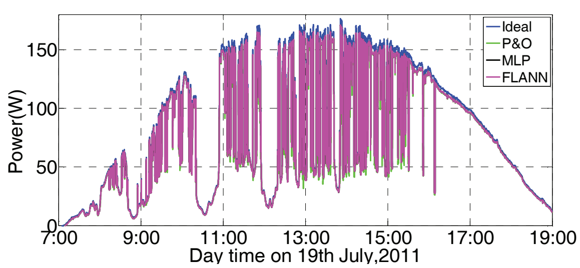

Fig. 6. Power by P&O, MLP and FLANN on 19 July, 2011.

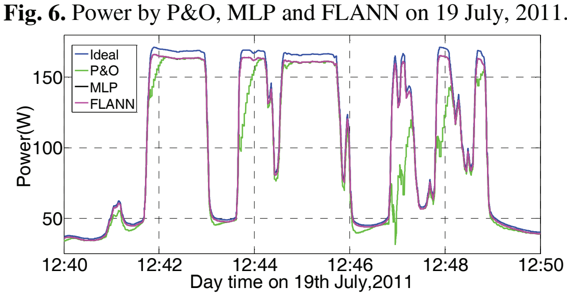

Fig.7. Blow up of Fig. 6 from 12:40pm to 12:50pm.

4. CONCLUSIONS AND FUTURE WORK

We proposed a novel FLANN-based controller for MPPT in PV system. Compared to other two traditional methods, P&O and MLP, it excels P&O for its ability to track MPP under rapidly changing conditions, and shows advantages over MLP in training time and computational complexity. By conducting three different experiments, better efficiency and lower power loss with FLANN controller are verified. Since FLANN structure reduces system complexity, it achieves relatively lower expense if implemented on hardware. In addition, it is important to point out that when under a long-term running, the accuracy of the prediction by the network can be improved by training the network after a certain running period. Our future work includes 1) implementing this algorithm in hardware, 2) investigating the intelligent methods to optimize the dimensions of the expanded inputs and considering MPPT issues under partially shaded conditions.

5. REFERENCES

[1] L. L. Buciarelli, B. L. Grossman, E. F. Lyon, and N. E. Rasmussen, "The energy balance associated with the use of a MPPT in a 100 kW peak power system," *in Proc. IEEE Photovoltaic Specialist Conf.*, pp. 523 - 527, 1980.

[2] J. J. Schoeman and J. D. Van Wyk, "A simplified maximal power controller for terrestrial photovoltaic panel arrays," *in Proc. IEEE Photovoltaic Specialist Conf.,* pp. 361 - 367, 1982.

[3] K. H. Hussein, I. Muta, T. Hoshino, and M. Osakada, "Maximum photovoltaic power tracking: an algorithm for rapidly changing atmospheric conditions," *in Proc. IEE Int'l Conf. on Generation, Transmission and Distribution*, vol. 142, no. 1, pp. 1350 - 2360, 1995.

[4] A. B. G. Bahgat, N. H. Helwa, G. E. Ahmad, and E. T. Shenawy, "Maximum power point tracking controller for PV systems using neural networks,"*Renewable Energy*,vol.30,no.8, pp. 1257-1268, 2005.

[5] T. L. Kottas, Y. S. Boutalis, and A. D. Karlis, "New maximum power point tracker for PV arrays using fuzzy controller in close cooperation with fuzzy cognitive networks, " *IEEE Trans. on Energy Conversion*, vol. 21, no. 2, pp. 793 - 803, 2006.

[6] T. Esram and P. L. Chapman, "Comparison of photovoltaic array maximum power point tracking techniques," *IEEE Trans. on Energy Conversion*, vol. 22, no. 2, pp. 439 - 449, 2007.

[7] J. C. Patra, L. L. Jiang and D. L. Maskell, "Estimation of external quantum efficiency for multi-junction solar cells under influence of charged particles using artificial neural networks," *in Proc. IEEE Int'l Conf. on SMC*, Alaska, USA, pp. 465 - 470, Oct. 2011.

[8] J. C. Patra, "Chebyshev neural network-based model for dual junction solar cells," *IEEE Trans. on Energy Conversion*, vol. 26, no. 1, pp. 132 - 139, 2011.

[9] J. C. Patra, "Neural network-based model for dual-junction solar cells," *Progress in Photovoltaics: Research and Applications*, vol. 19, no. 1, pp. 33 - 44, 2011.

[10] J. C. Patra, and D. L. Maskell, "Artificial neural network- based model for estimation of EQE of multi-junction solar cells, " *in Proc. IEEE Photovoltaic Specialists Conf.*, Seattle, USA, June 2011.

[11] J. C. Patra, and D. L. Maskell, "Estimation of dual-junction solar cell characteristics using neural networks," *in Proc. IEEE Photovoltaic Specialists Conf.*, Honolulu, USA, pp. 2709 - 2713, June 2010.

[12] K. Ishaque, Z. Salam, and H. Taheri, "Accurate MATLAB simulink PV system simulator based on a two-diode model," *Journal of Power Electronics*, vol. 11, no. 2, pp. 179 - 187, 2011.

[13] J. C Patra, R. N. Pal and B. N. Chatterji, "Identification of non-linear dynamic systems using functional link artificial neural networks," *IEEE Trans. on Systems, Man, and Cybernetics,* vol. 29, no. 2, pp. 254 - 262, 1999.